Liquid-phase and solid-phase microwave irradiations for reduction of graphite oxide*

Zhao Na(赵 娜)[a], Wen Chen-Yu(文宸宇)[a], Zhang David Wei(张 卫)[a], Wu Dong-Ping(吴东平)[a]†, Zhang Zhi-Bin(张志滨)[b], and Zhang Shi-Li(张世理)[b]

[a] *State Key Laboratory of ASIC and System, Fudan University, Shanghai* 200433, *China*

[b] *Solid-State Electronics, The Ångström Laboratory, Uppsala University, P. O. Box* 534, 75121 *Uppsala, Sweden*

(Received 24 February 2014; revised manuscript received 21 June 2014; published online 10 October 2014)

In this paper, two microwave irradiation methods: (i) liquid-phase microwave irradiation (MWI) reduction of graphite oxide suspension dissolved in de-ionized water and N, N-dimethylformamide, respectively, and (ii) solid-phase MWI reduction of graphite oxide powder have been successfully carried out to reduce graphite oxide. The reduced graphene oxide products are thoroughly characterized by scanning electron microscopy, atomic force microscopy, X-ray photoelectron spectroscopy, Fourier transform infrared spectral analysis, Raman spectroscopy, UV-Vis absorption spectral analysis, and four-point probe conductivity measurements. The results show that both methods can efficiently remove the oxygen-containing functional groups attached to the graphite layers, though the solid-phase MWI reduction method can obtain far more efficiently a higher quality-reduced graphene oxide with fewer defects. The $I(D)/I(G)$ ratio of the solid-phase MWI sample is as low as 0.46, which is only half of that of the liquid-phase MWI samples. The electrical conductivity of the reduced graphene oxide by the solid method reaches 747.9 S/m, which is about 25 times higher than that made by the liquid-phase method.

Keywords: microwave irradiation, solid-phase, liquid-phase, reduced graphene oxide

PACS: 81.05.–t, 81.05.U–, 81.05.ue **DOI:** 10.1088/1674-1056/23/12/128101

1. Introduction

Graphene, a two-dimensional material, has attracted tremendous attention in recent years for its excellent mechanical strength, thermal stability, optical properties,[1–8] high intrinsic carrier mobility at room temperature, and potential applications in nano-electronics and devices.[9] In the past, extensive work on the preparation of graphene by solid or liquid methods has been conducted, including chemical vapor deposition,[10–13] mechanical exfoliation,[5] chemical redox,[14] epitaxial growth on SiC,[15,16] and organic synthesis.[17] The reduced graphene oxide (RGO), typically made from inexpensive graphite through the chemical redox method, has been widely adopted for preparing the large scale production of RGO. However, the resulting RGO products are not easily purified, and it has been demonstrated that the presence of residual oxygen, owing to an incomplete reaction or the reactant itself, remarkably hampers the carrier transport in the graphitic lattice.[17]

Microwave irradiation (MWI) has recently come into being as an alternative method of reducing and exfoliating the graphite oxide (GO).[9,18] The MWI has been widely used as a rapid heating source in the presence of microwave susceptor.[19–22] MWI has also been reported being used for synthesizing soluble single wall carbon nanotube derivatives.[23] Compared with conventional chemical redox methods, the MWI method has advantages of shorter preparation time and lower cost, and thus is potentially more suitable for large scale production of RGO.

Microwave-assisted reduction of GO can be conducted in either a solid-phase or liquid-phase environment. High quality graphene nanosheets produced by solid-phase microwave irradiation under a hydrogen atmosphere have been reported by Park *et al.*[21] Recently, microwave-assisted chemical reduction of GO has been realized by heating GO suspensions in aqueous or organic media.[9,24] For example, Wang *et al.*[24] have developed a facile and environment-friendly method to reduce GO in ionic liquids by liquid-phase microwave-assisted ionothermal treatment.[24]

Although previous work has reported the feasibility of using MWI for the reduction of GO, the direct comparison between different MWI methods has not been carefully studied. In this paper, we employed both liquid-phase and solid-phase MWI reduction methods for reducing GO. For the liquid-phase MWI reduction methods, de-ionized water and typical polar organic N, N-dimethylformamide (DMF) are used as the solvents respectively, whereas for the solid-phase MWI reduction method, the GO powder is directly microwave irradiated under a nitrogen atmosphere. Comprehensive comparisons between the solid-phase and liquid-phase MWI methods are obtained through a series of characterization means and thorough anal-

*Project supported by the National Natural Science Foundation of China (Grant No. 61176090) and the National Science and Technology Project 02, China (Grant No. 2013ZX02303-004).

†Corresponding author. E-mail: dongpingwu@fudan.edu.cn

© 2014 Chinese Physical Society and IOP Publishing Ltd

ysis.

2. Experimental procedures

2.1. Materials

All materials were obtained from commercial sources. GO was purchased from Nanjing XianFeng Nano Co. Ltd. China; N,N-dimethyl-formamide (DMF) (analytical reagent grade) was supplied by Sinopharm Chemical Reagent Co. Ltd. China. Deionized water was made by Elix 3 (Milli Pore Co. Ltd. USA), and its resistivity was higher than 18 MΩ·cm.

2.2. Reduction

Experimentally, the GO, with de-ionized water as the solvent, was sonicated by a pin ultrasonic system for 15 min. Then, the suspension was transferred into a quartz tube and microwave irradiated in a 100-W microwave oven (Discover, CEM, USA) for 30 min. After the reaction, the yellow dispersion of the GO suspension turned totally dark, and hence the RGO through liquid-phase MWI was obtained. The sample, hereafter, is named RGO-MWI-water. For comparison, the sample, with DMF as the solvent, (RGO-MWI-DMF) was also prepared using identical sample treatments.

To obtain the reduced graphene oxide made using the solid-phase MWI method (RGO-MWI), 100-mg GO was placed in a quartz vessel and then irradiated at 5.8-GHz for 10 min in a MWI annealing system (AXOM 200, DSGI Technologies, USA); the MWI power level was 1400 W. Nitrogen cover gas with a flow of 20 sccm in the volume of 0.785 m^3 was utilized. Inspection after the irradiation revealed that the GO was reduced to dark flocculent RGO.

For both the liquid-phase and solid-phase MWI processes, a series of process conditions have been conducted for the sake of optimization and adequate comparison. The aforementioned process parameters were chosen under the optimization criteria that the processed GO have fully turned into RGO and the effect of MWI becomes relatively saturated, which is evidenced by the complete color change (from yellow or brown to deep dark) and a substantial decrease of the characteristic peaks by Fourier transform infrared spectroscopy (FT-IR) of the RGO samples. The as-obtained RGO samples were characterized by scanning electron microscopy (SEM; Hitachi, SU1510, Japan), atomic force microscopy (AFM, MultiMode, Veeco Co. Ltd. USA), FT-IR (Nicolet 6700, Thermo Fisher Co. Ltd. USA), X-ray photoelectron spectroscopy (XPS; Axis Ultra DLD, Kratos, UK), Raman spectroscopy (inVia, Renishaw Co. Ltd. UK; equipped with a 514-nm wavelength laser), X-ray diffraction analysis (XRD, D/Max-2400, Rigaku, Japan), transmission ultraviolet-visible spectral analysis (UV-vis, Lambda 750S, Perkin Elmer, USA) and the four-point probe method (SDY-4, 4PROBES TECH Co. Ltd. China).

3. Results and discussion

The morphological features of the GO film prepared by the suspension and ultrasonic dispersion method are studied by SEM and the micrograph is shown in Fig. 1(a). SEM images of the three RGO samples that are obtained from the liquid-water, liquid DMF, and solid-phase MWI methods are shown in Figs. 1(b)–1(d), respectively. For all three RGO samples, transparent and wrinkled sheets are present, indicating that in each case, a successful reduction of GO to graphene nanosheets is achieved. The AFM images and the section profiles of the GO and RGO samples are shown in Fig. 2. The measured thickness values of the graphene flakes exfoliated from the GO samples range from 0.8 nm to 1.2 nm, indicating that the graphene sheets in the RGO samples are stacked into one or several layers.

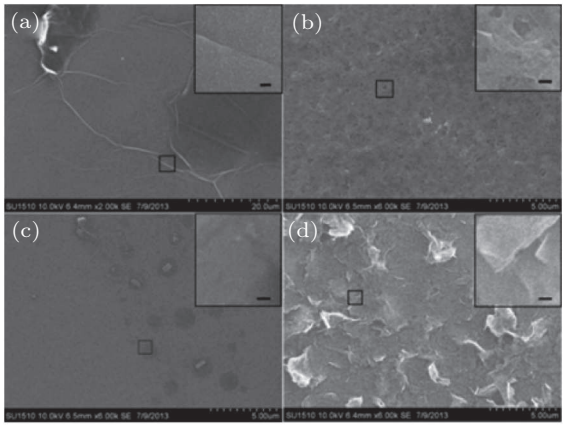


Fig. 1. SEM images of (a) GO after ultrasonic dispersion, (b) RGO-MWI-water, (c) RGO-MWI-DMF, and (d) RGO-MWI. (High-resolution SEM image of each of the samples is shown in the corresponding inset.)

Epoxy, carbonyl, and hydroxyl groups are the main oxygen-containing functional groups attached to GO layers,[25] therefore, the effectiveness in removing these groups is the key criteria for GO reduction. In turn, we will review the various analytical methods and describe our observations.

FT-IR spectral analysis provides an overall indication of the reduction level of the RGO samples prepared by different reduction methods. As shown in Fig. 3, for the RGO-MWI sample, almost no absorption peak can be seen in the FT-IR spectra, indicating that almost complete removal of the oxygen-containing functional groups attached to the RGO-MWI sample has occurred. In contrast, after reduction, for the liquid-phase water and DMF samples, characteristic peaks such as the C=O (1735 cm^{-1}), carboxyl C–O

(1400 cm^{-1}), epoxy C–O (1228 cm^{-1}),[26] and aromatic C=C (1577 cm^{-1})[21,22] are still discernable. The remaining hydroxyl groups (2900 cm^{-1}–3600 cm^{-1}) on the liquid-phase water samples may be related to the assumption that reduction of carbonyl or epoxy groups in water is achieved in two steps: first turning to –OH, and then reducing to H_2O and graphene with sp^2-bonded carbon atoms[27] as demonstrated by the "aromatic" peak associated with the RGO-MWI-water sample. Moreover, in the liquid-phase MWI method with water as the solvent, the reduction of the –OH groups may not be so easy as in the solid-phase MWI method, because the reaction product H_2O cannot be easily drained away.

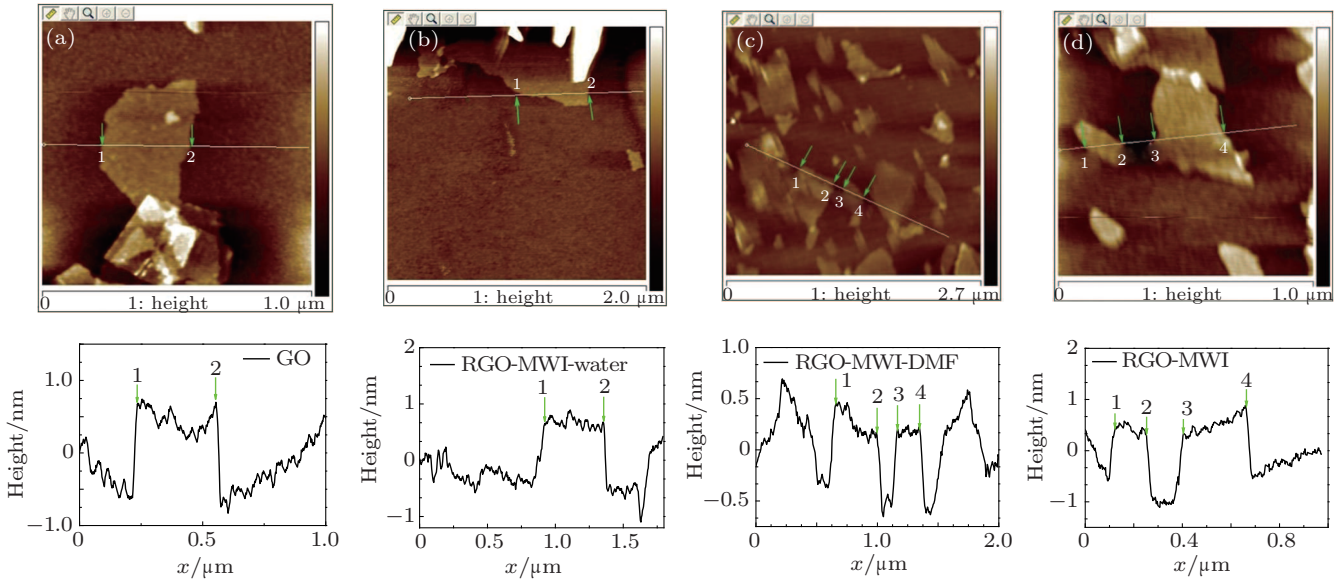


Fig. 2. (color online) AFM images and the section profiles of (a) GO, (b) RGO-MWI-water, (c) RGO-MWI-DMF, and (d) RGO-MWI.

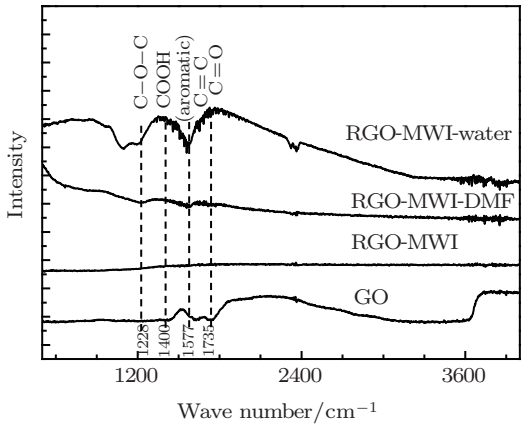


Fig. 3. FT-IR spectra of the GO and RGO samples.

XPS spectroscopy is suitable for the evaluation of the material compositions and decomposition of the C1s XPS spectrum into its main components can help understand the reduction processes. The C1s XPS spectra of the GO and RGO samples are shown in Figs. 4(a)–4(d). The binding energy peak at 284.6 eV is attributed to the C=C bonds, and the peaks at 285.6, 286.6, 287.7, and 288.7 eV are typically assigned to the hydroxyl, epoxy, C=O, and –COOH functional groups respectively.[14,24] A new peak appeared at 291.5 eV, which is attributed to the π–π^* shake-up of aromatic or conjugated system.[28] Compared to the GO sample, all the three RGO samples exhibit significantly weaker intensities of the oxygen-containing functional groups, proving that a de-oxygenation process has occurred. For the sake of verification and comparison with FT-IR results, hydroxyl proportions among oxygen-containing groups are also obtained based on the calculations of the areas of all oxygen-containing functional groups in C1s XPS spectra. The percentages of hydroxyl are calculated to be 46.0% in RGO-MWI-water, 70.1% in RGO-MWI-DMF, and only 12.2% in RGO-MWI. Hence, it can be inferred that hydroxyl groups have been almost removed in the solid-phase MWI reduction process, which is also observed in the aforementioned FT-IR results.

The carbon/oxygen (C/O) atom ratio is calculated from the areas of the C1s and O1s peaks, and their relative atomic sensitivity factors. It is a macroscale feature used to evaluate the overall level of RGO sample reduction. As shown in Fig. 4(e), the C/O ratios of the RGO-MWI-water, RGO-MWI-DMF, and RGO-MWI samples are 6.60, 6.13, and 7.24, respectively, while the C/O ratio of the GO sample is merely 2.13. This significant increase in the C/O ratio after MWI is attributed to the effective reduction of GO after the treatment. Furthermore, the RGO-MWI sample has the highest C/O ratio despite the relatively low power density and short irradiation time.

Raman spectroscopy is also able to provide information about the structural properties such as disorder and defect structures of the carbonaceous materials.[22] Figure 5 shows

the Raman spectra of the GO and RGO samples. Each sample has two characteristic peaks: 1350 cm^{-1} (D band) and 1580 cm^{-1} (G band).[19–22,29] The D band is related to the disorder-induced mode associated with structural defects and imperfections, while the G band reflects the first-order scattering of the E_{2g} mode from the sp^2 carbon domains and degree of crystallinity.[30] Generally, the intensity ratio of the D peak to G peak ($I[D]/I[G]$) is used as a measure to evaluate the quality of the graphitic structure, because this ratio approaches to zero for highly ordered pyrolytic graphite,[9,22] an increase of the $I(D)/I(G)$ means the degradation of crystallinity of the graphitic materials. The $I(D)/I(G)$ ratios for all the samples are provided in Table 1. Both the RGO-MWI-water and RGO-MWI-DMF samples have slightly reduced $I(D)/I(G)$ ratios compared with the GO sample. Note, the RGO-MWI sample has a significantly lower $I(D)/I(G)$ value than the other samples. It is known that the $I(D)/I(G)$ value usually increases after reduction using chemical redox methods,[31] indicating that the chemical redox reaction introduces new defects rather than the restoration of the original ones. Hence, it may be inferred that the solid-phase MWI method is more advantageous in repairing lattice imperfections than the liquid-phase MWI or conventional chemical redox methods.

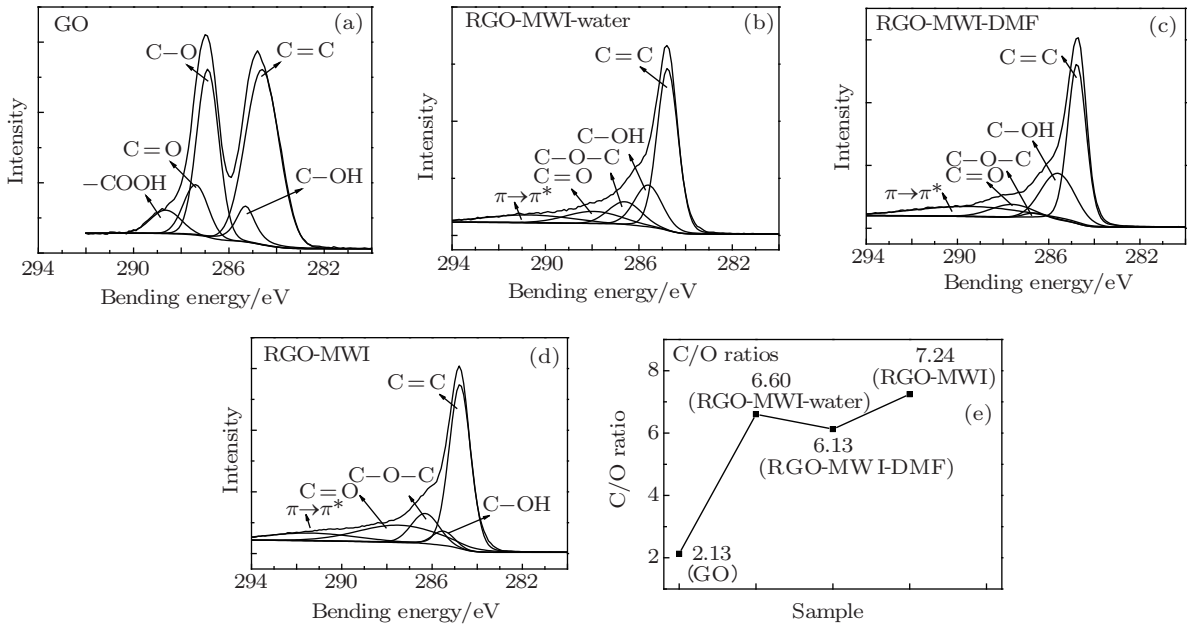


Fig. 4. High-resolution C1s XPS spectra and C/O ratios of the samples. (a) GO, (b) RGO-MWI-water, (c) RGO-MWI-DMF, (d) RGO-MWI, and (e) C/O atom ratio values, obtained by XPS analysis for the GO and RGO samples.

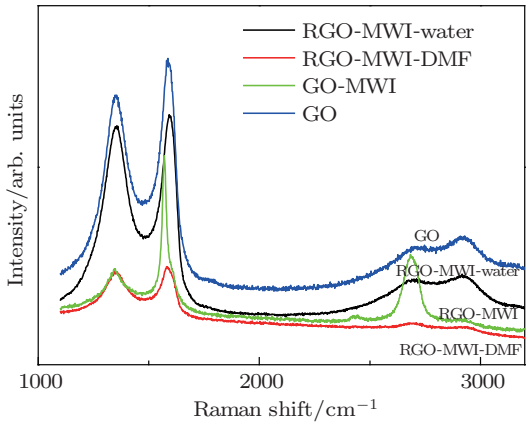


Fig. 5. (color online) Raman spectra of the GO and RGO samples after reduction by different methods.

Table 1. Raman spectroscopy-derived $I(D)/I(G)$ ratios of the samples.

Sample	RGO-MWI-water	RGO-MWI-DMF	RGO-MWI	GO
$I(D)/I(G)$	0.88	0.95	0.46	0.96

Reduction of GO to RGO should be accompanied with structural changes, especially the change in the distances between various atomic layers.[27] To verify this fact, the microstructures of the samples are characterized by XRD with Cu K_α radiation ($\lambda = 1.5418$ Å). XRD scans show that the interlayer distance of the RGO film (Fig. 6) decreases from 8.10 Å ($2\theta = 10.9°$) to about 6.6 Å ($2\theta = 13.4°$) for the original GO film. As the RGO films were prepared on top of the silicon substrates, the sharp peak at $2\theta = 33°$ in the RGO-MWI sample is supposed to be the characteristic peak of silicon (400) according to calculations by the PDF cards. The reduction of the interlayer distance is likely attributed to the elimination of the covalently bound oxygen-containing groups between the GO interlayers. The disappearance of the peak at 10.9° in the XRD pattern for the MWI reduced samples confirms that efficient reduction of the GO sheets is achieved for

each of all of the MWI-treated RGO samples.[9]

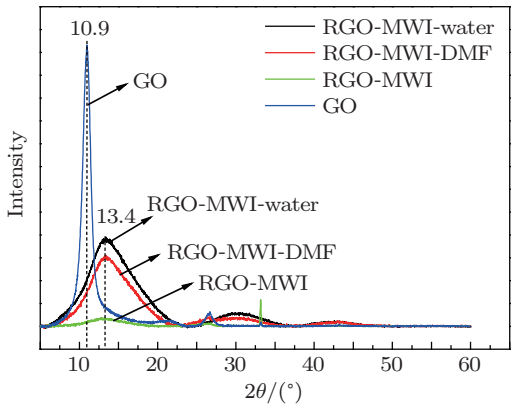


Fig. 6. (color online) XRD scans of the GO and RGO samples after reduction by different methods.

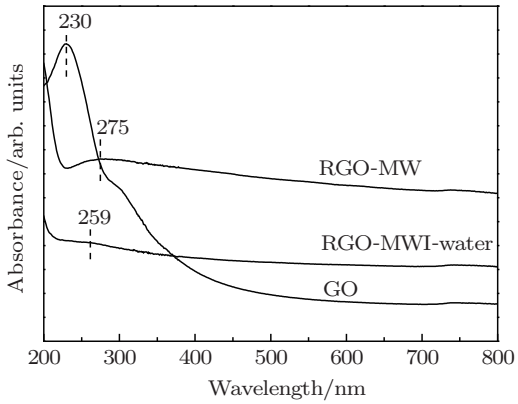


Fig. 7. UV-vis absorption spectra of the GO and RGO samples.

UV-vis absorption spectroscopy is also often used to evaluate the level of reduction for RGO sheets.[32] UV-vis spectra of the GO, RGO-MWI, and RGO-MWI-water samples are measured by using aqueous solutions in optically transparent cuvettes. The data for the RGO-MWI-DMF sample are not shown here because DMF has a strong absorption beyond 300 nm and this masks the RGO absorption peak. As shown in Fig. 7, the maximum absorption peak at 230 nm, which corresponds to the π–π^* transition of aromatic C–C bonds in the GO sample, shifts to 259 nm and 275 nm after having been reduced by MWI-water and MWI, respectively. This shift represents the gradual restoration of the p-conjugation network within the graphene sheets[22,33] during MWI treatment. The shoulder (at 300 nm) observed in the GO sample is attributed to the n–π^* transitions of the C=O bonds[24–29] and this is not present in the RGO sample, suggesting that the efficient removal of C=O is achieved for the RGO sample.

The electrical conductivities of the RGO samples are directly related to their electron mobilities, which are determined by the number of oxygen-containing functional groups and the level of defects in the graphene skeleton. The conductivities of the GO and RGO samples (shown in Table 2) are determined using the four-point resistivity values that are extracted from the measured sheet resistances and the thickness values of the RGO films. Since it is difficult to form paper-like thin films for the GO and RGO-MWI-water samples, the nominal conductivity value provided by the GO material supplier is used for the GO sample. The conductivity value for RGO-MWI-water is not available (NA).

Obviously, after the reduction, both the RGO-MWI-DMF and the RGO-MWI samples have significantly high conductivity levels compared with the original GO sample, proving the effectiveness of both the liquid-phase and solid-phase MWI methods of reducing GO to RGO holds. However, the conductivity of RGO-MWI is almost 25 times higher than that of RGO-MWI-DMF (747.9 S/m versus 29.9 S/m). It is a commonly known fact that crystallographic disorder and defects in the graphene skeleton strongly reduce its electron mobility. Moreover, the defects in the form of carbon vacancies cannot be healed by the chemical reduction process.[34] Hence the large difference in conductivity values between the RGO-MWI-DMF and RGO-MWI samples indicates that the solid-phase MWI leads to a much enhanced capability in healing the lattice imperfections of the graphene skeletons compared with the scenario of liquid-phase MWI. This finding is consistent with aforementioned results obtained from Raman spectra where the RGO-MWI sample exhibits a much lower $I(D)/I(G)$ ratio than the two liquid-phase MWI samples.

Table 2. Electrical conductivities of the samples.

Sample	RGO-MWI-water	RGO-MWI-DMF	RGO-MWI	GO
Conductivity/(S/m)	NA	29.9	747.9	0.034

The reduction mechanisms and the differences among the three MWI samples can be tentatively explained by the following perspectives. The level of the liquid-phase MW reduction relies mainly on the efficiency of the interaction between the molecules in a reaction mixture and the electromagnetic waves.[35] For the liquid-phase MWI water and DMF methods, the reduction of the GO is assumed to be dominated by the thermal effect from the surrounding liquid water and DMF. Both water and DMF can absorb microwave energy with a high efficiency, which is attributed to their highly polarized molecular structures. Furthermore, due to the retardation of nucleation under microwave heating, the solvents may be super-heated beyond their normal boiling-points. Consequently, the GO can be effectively reduced by the liquid-

phase MWI water and DMF methods compared with under conventional heating.[35] For the solid-phase MWI, the reduction of GO depends greatly on the local-thermal effect caused by the strong interaction between the highly polarized oxygen-containing functional groups and the supplied microwaves. This can result in local flash-heating, and the local temperature has been reported to reach instantly as high as 1500 °C when microwave arcing occurred.[21] Hence, the local temperature of the solid-phase MWI GO sample can greatly exceed the temperatures of the super-heated liquid-phase MWI water and DMF GO samples. Consequently, the solid-phase MWI method is much more efficient to remove the oxygen-containing functional groups and heal the defects in the graphene skeleton. Namely, compared with liquid-phase MWI, solid-phase MWI has the advantage of having a high local-thermal effect and is therefore able to achieve a substantially high reduction level. Besides, the solid-phase MWI method can provide a much reduced process time compared with the liquid-phase MWI methods.

4. Conclusions

In this work, two liquid-phase methods and a solid-phase MWI method are used to reduce GO. A series of analytical techniques is used to evaluate the quality of these reductions. Results show that the two liquid-phase MWI methods and the solid-phase MWI method are able to effectively remove most of the oxygen-containing functional groups from the graphite oxide samples, resulting in only a few lattice defects. However, solid-phase MWI demonstrates clear advantages in the restoration of RGO lattice imperfections because of the direct and strong interaction between GO and the microwaves. More importantly, based on our experimental evidence (electrical conductivity in particular), the solid-phase MWI method provides a most promising method of manufacturing cost-effective, high-throughput, and high-quality RGO materials.

References

[1] Gómez-Navarro C, Weitz R T, Bittner A M, Scolari M, Mews A, Burghard M and Kern K 2007 *Nano Lett.* **7** 3499

[2] Gilje S, Han S, Wang M, Wang K L and Kaner R B 2007 *Nano Lett.* **7** 3394

[3] Geim A K and Novoselov K S 2007 *Nat. Mater.* **6** 183

[4] Liang X, Fu Z and Chou S Y 2007 *Nano Lett.* **7** 3840

[5] Novoselov K S, Geim A K, Morozov S V, Jiang D, Zhang Y, Dubonos S V, Grigorieva I V and Firsov A A 2004 *Science* **306** 666

[6] Watcharotone S, Dikin D A, Stankovich S, Piner R, Jung I, Dommett G H B, Evmenenko G, Wu S E, Chen S F, Liu C P, Nguyen S T and Ruoff R S 2007 *Nano Lett.* **7** 1888

[7] Eda G, Fanchini G and Chhowalla M 2008 *Nat. Nanotechnol.* **3** 270

[8] Blake P, Brimicombe P D, Nair R R, Booth T J, Jiang D, Schedin F, Ponomarenko L A, Morozov S V, Gleeson H F, Hill E W, Geim A K and Novoselov K S 2008 *Nano Lett.* **8** 1704

[9] Hassan H M A, Abdelsayed V, Khder A E R S, AbouZeid K M, Terner J, El-Shall M S, Al-Resayes S I and El-Azhary A A 2009 *J. Mater. Chem.* **19** 3832

[10] Ambrosi A and Pumera M 2013 *J. Phys. Chem. C* **117** 2053

[11] Li X S, Cai W W, An J H, Kim S Y, Nah J H, Yang D X, Piner R, Velamakanni A, Jung I, Tutuc E, Banerjee K S, Colombo L and Ruoff R S 2009 *Science* **324** 1312

[12] Ren W C, Gao L B, Ma L P and Cheng H M 2011 *New Carbon Mater.* **26** 71

[13] Kim K S, Zhao Y, Jang H, Lee S Y, Kim J M, Kim K S, Ahn J H, Kim P, Choi J Y and Hong B H 2009 *Nature* **457** 706

[14] Fernández-Merino M J, Guardia L, Paredes J I, Villar-Rodil S, Solís-Fernández P, Martínez-Alonso A and Tascón J M D 2010 *J. Phys. Chem. C* **114** 6426

[15] Wang D C, Zhang Y M, Zhang Y M, Lei T M, Guo H, Wang Y H, Tang X Y and Wang H 2011 *Chin. Phys. B* **20** 128101

[16] Wang D C, Zhang Y M, Zhang Y M, Lei T M, Guo H, Wang Y H, Tang X Y and Wang H 2012 *Chin. Phys. B* **21** 038102

[17] Simpson C D, Mattersteig G, Martin K, Gherghel L, Bauer R E, Räder H J and Müllen K 2004 *J. Am. Chem. Soc.* **126** 3139

[18] Zhu Y W, Murali S, Stoller M D, Velamakanni A, Piner R D and Ruoff R S 2010 *Carbon* **48** 2118

[19] Paton K R and Windle A H 2008 *Carbon* **46** 1935

[20] Imholt T J, Dyke C A, Hasslacher B, Perez J M, Price D W, Roberts J A, Scott J B, Wadhawan A, Ye Z and Tour J M 2003 *Chem. Mater.* **15** 3969

[21] Park S H, Bak S M, Kim K H, Jegal J P, Lee S I, Lee J and Kim K B 2011 *J. Mater. Chem.* **21** 680

[22] Zhu C Z, Guo S J, Fang Y X and Dong S J 2010 *ACS Nano* **4** 2429

[23] Negra F D, Meneghetti M and Menna E 2003 *Fullerenes, Nanotubes and Carbon Nanostructures* **11** 25

[24] Wang B G, Wang X B, Lou W J and Hao J C 2012 *New J. Chem.* **36** 1684

[25] Gao W, Alemany L B, Ci L and Ajayan P M 2009 *Nat. Chem.* **1** 403

[26] Chen W F and Yan L F 2010 *Nanoscale* **2** 559

[27] Liao K H, Mittal A, Bose S, Leighton C, Mkhoyan K A and Macosko C W 2011 *ACS Nano* **5** 1253

[28] Fan X B, Peng W C, Li Y, Li X Y, Wang S L, Zhang G L and Zhang F B 2008 *Adv. Mater.* **20** 4490

[29] Glover A J, Cai M, Overdeep K R, Kranbuehl D E and Schniepp H C 2011 *Macromolecules* **44** 9821

[30] Zangmeister C D 2010 *Chem. Mater.* **22** 5625

[31] Shin H J, Kim K K, Benayad A, Yoon S M, Park H K, Jung I S, Jin M H, Jeong H K, Kim J M, Choi J Y and Lee Y H 2009 *Adv. Func. Mater.* **19** 1987

[32] Williams G, Seger B and Kamat P V 2008 *ACS Nano* **2** 1487

[33] Lei Z B, Lu L and Zhao X S 2012 *Energy & Environ. Sci.* **5** 6391

[34] López V, Sundaram R S, Gómez-Navarro C, Olea D, Burghard M, Gómez-Herrero J, Zamora F and Kern K 2009 *Adv. Mater.* **21** 4683

[35] Vivek P, Rajender S V 2010 *Aqueous Microwave Assisted Chemistry Synthesis and Catalysis* (Cambridge: Royal Society of Chemistry) pp. 4–8